ADVANCED SCIENCE
Open Access

Supporting Information

for *Adv. Sci.*, DOI 10.1002/advs.202206007

The Imbalance of p53–Park7 Signaling Axis Induces Iron Homeostasis Dysfunction in Doxorubicin-Challenged Cardiomyocytes

Jianan Pan, Weiyao Xiong, Alian Zhang, Hui Zhang, Hao Lin, Lin Gao, Jiahan Ke, Shuying Huang, Junfeng Zhang, Jun Gu, Alex Chia Yu Chang* and Changqian Wang**

Supporting Information

The Imbalance of p53-Park7 Signaling Axis Induces Iron Homeostasis Dysfunction in Doxorubicin-Challenged Cardiomyocytes

Table S1 Sequences of gene-shRNA

shRNA	**Sequence**
sh*Park7*-1	GCAGTGTAGCCGTGATGTAAT
sh*Park7*-2	GAAATCTGGGTGCACAGAATT
sh*Park7*-3	GCTCTGTTGGCTCACGAAGTA
Scramble	UUCUCCGAACGUGUCACGUTT

Table S2 Antibodies.

Antibodies	**Cat. No. and Company**	**Dilution Ratio**
cTnT	ab8295, Abcam	1:200 for IF
TfR	ab214039, Abcam	1:1000 for WB
FPN	26601-1-AP, Proteintech	1:1000 for WB
FTH	sc-376594, Santa Cruz Biotechnology	1:500 for WB
IRP1	sc-166022, Santa Cruz Biotechnology	1:500 for WB
IRP2	23829-1-AP, Proteintech	1:1000 for WB
MFRN	26469-1-AP, Proteintech	1:1000 for WB
Park7	5933, Cell Signaling Technology	1:1000 for WB; 1:100 for IF; 1μg/mg protein for IP
p53	2524, Cell Signaling Technology	1:1000 for WB; 1μg/mg protein for IP

p53	10442-1-AP, Proteintech	1:1000 for WB
GAPDH	60004-1-Ig, Proteintech	1:10000 for WB
HSP60	15282-1-AP, Proteintech	1:10000 for WB
Normal Rabbit IgG	2729, Cell Signaling Technology	1μg/mg protein for IP
Normal Mouse lgG	B900620, Proteintech	1μg/mg protein for IP
Anti-mouse IgG (H+L) (DyLight™ 800 4X PEG Conjugate)	5257, Cell Signaling Technology	1:30000 for WB
Anti-rabbit IgG (H+L) (DyLight™ 800 4X PEG Conjugate)	5151, Cell Signaling Technology	1:30000 for WB
Anti-rabbit IgG (H+L), F(ab')2 Fragment (Alexa Fluor® 594 Conjugate)	8889, Cell Signaling Technology	1:1000 for IF

Anti-mouse IgG (H+L), F(ab')2 Fragment (Alexa Fluor® 488 Conjugate)	4408, Cell Signaling Technology	1:1000 for IF
Anti-mouse IgG (H+L), F(ab')2 Fragment (Alexa Fluor® 594 Conjugate)	8890, Cell Signaling Technology	1:1000 for IF

Table S3 Primers for real-time PCR.

Primers	**Sequences 5'---3'**
Mouse *Ptgs2* Fw	CTGCGCCTTTTCAAGGATGG
Mouse *Ptgs2* Re	GGGGATACACCTCTCCACCA
Mouse *Park7* Fw	AGTCGCCTATGGTGAAGGAGATCC
Mouse *Park7* Re	TGAGCCAACAGAGCCGTAGGAC
Mouse *p53* Fw	AGTAAAGGCTCTAAAGCTCACCC
Mouse *p53* Re	CCCATCGTCAACTTGGTCCA
Mouse *Gapdh* Fw	ATCATCCCTGCATCCACT
Mouse *Gapdh* Re	ATCCACGACGGACACATT

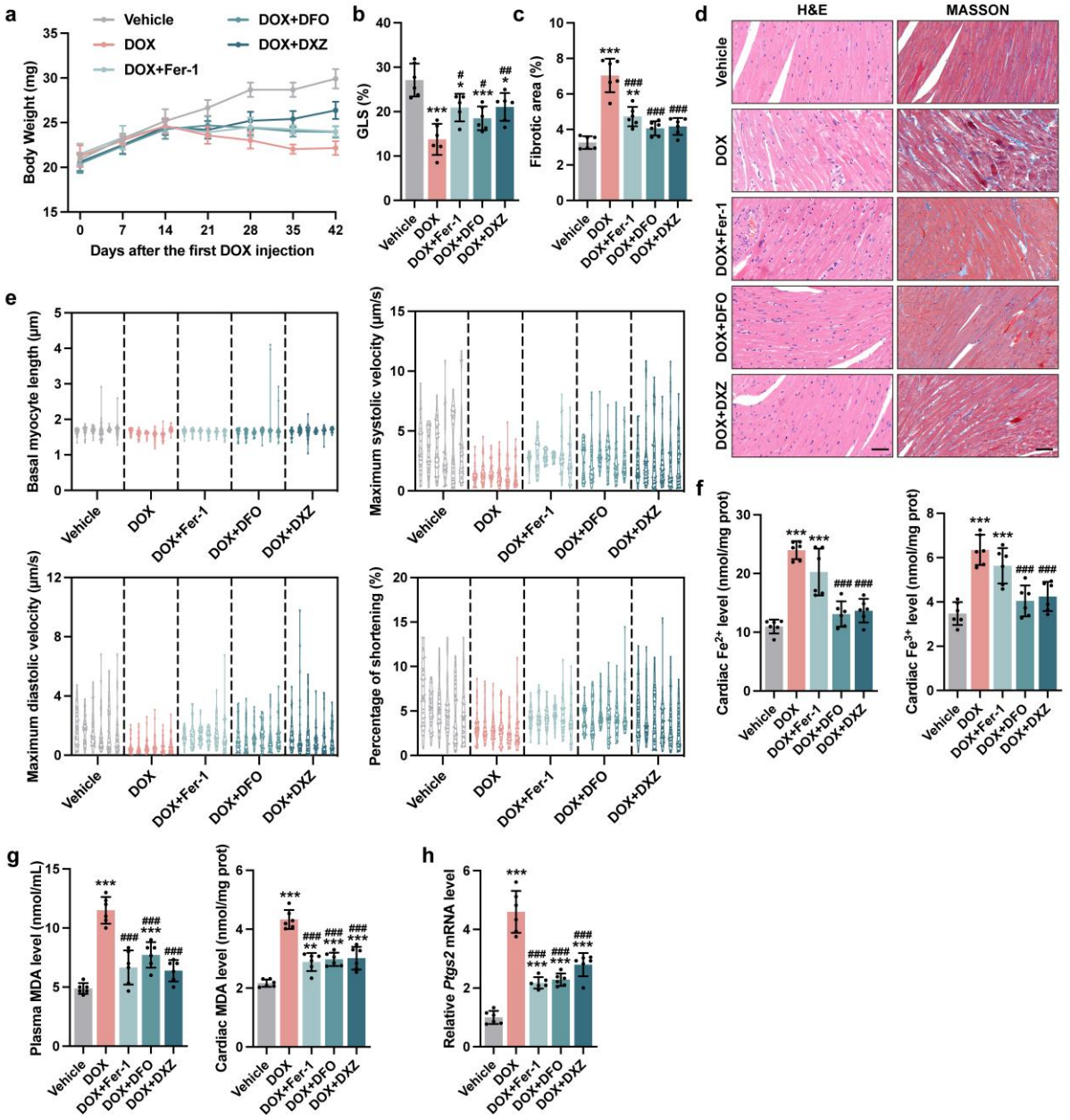

Figure S1 Blocking myocardial ferroptosis significantly alleviates DoIC *in vivo*.

a) Body weight tracing during DoIC model (n = 10). **b)** Quantification of global longitudinal strain (GLS; n=6). **c)** Percentage of fibrotic area in heart sections (n = 6). **d)** Representative micrographs of H&E and Masson's trichrome staining in heart sections (scale bars, 50 μm). **e)** Calculation of basal myocyte length, maximum systolic velocity, maximum diastolic velocity and percentage of shortening of AMCMs of each mouse (n = 30 AMCMs per mouse). **f)** Fe^{2+}

and Fe^{3+} levels in heart tissues (n = 6). **g)** MDA level in plasma and heart tissues (n = 6). **h)** *Ptgs2* mRNA expression in AMCMs (n = 6). The data are expressed as mean ± SD and analyzed using one-way ANOVA followed by Tukey's post hoc test, *$p < 0.05$, **$p < 0.01$ and ***$p < 0.001$ vs. Vehicle group; #$p < 0.05$, ##$p < 0.01$ and ###$p < 0.001$ vs. DOX group.

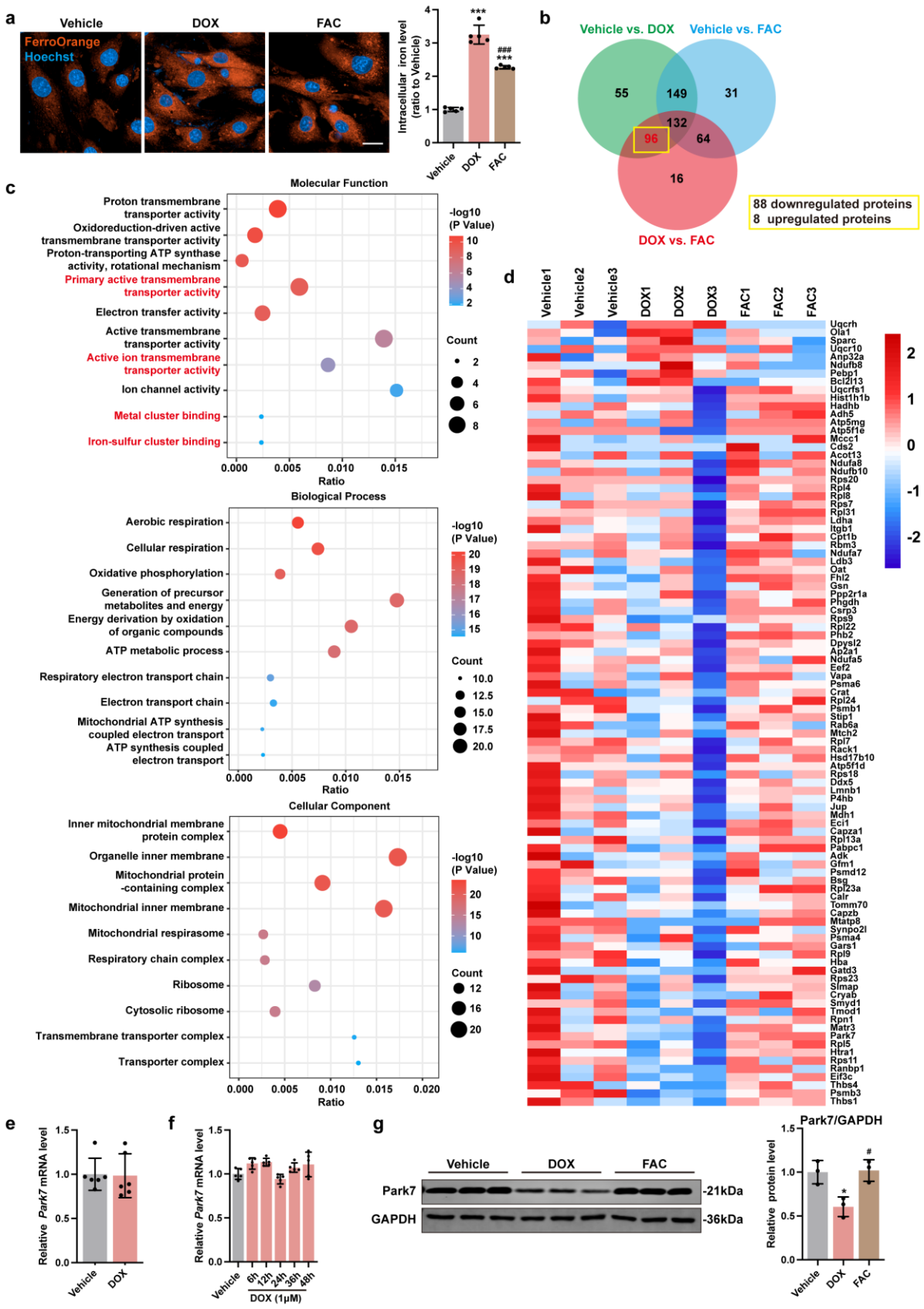

Figure S2 DOX impairs iron homeostasis in cardiomyocytes which is associated with

Park7 downregulation.

a) Representative micrographs and quantitative analysis of intracellular iron level (FerroOrange staining) (scale bars, 20 μm; n = 5). **b)** Venn analysis of differentially expressed proteins in NMCMs (Proteins of a 1.2-fold change (≥1.2 or ≤0.83) of Coverage without $P < 0.05$ cutoff). **c)** Gene ontology analysis of differentially expressed proteins. **d)** Heatmap of DOX-dysregulated proteins. **e)** *Park7* mRNA expression in AMCMs from chronic mice DoIC model (n = 6). **f)** *Park7* mRNA expression in NMCMs treated with 1 μM DOX in different times (n = 5). g) Representative immunoblots and quantitative analysis of Park7 in NMCMs treated with DOX or FAC (n = 3). The data are expressed as mean ± SD and analyzed using Student's t-test and one-way ANOVA followed by Tukey's post hoc test, ***$p < 0.001$ vs. Vehicle group; ###$p < 0.001$ vs. DOX group.

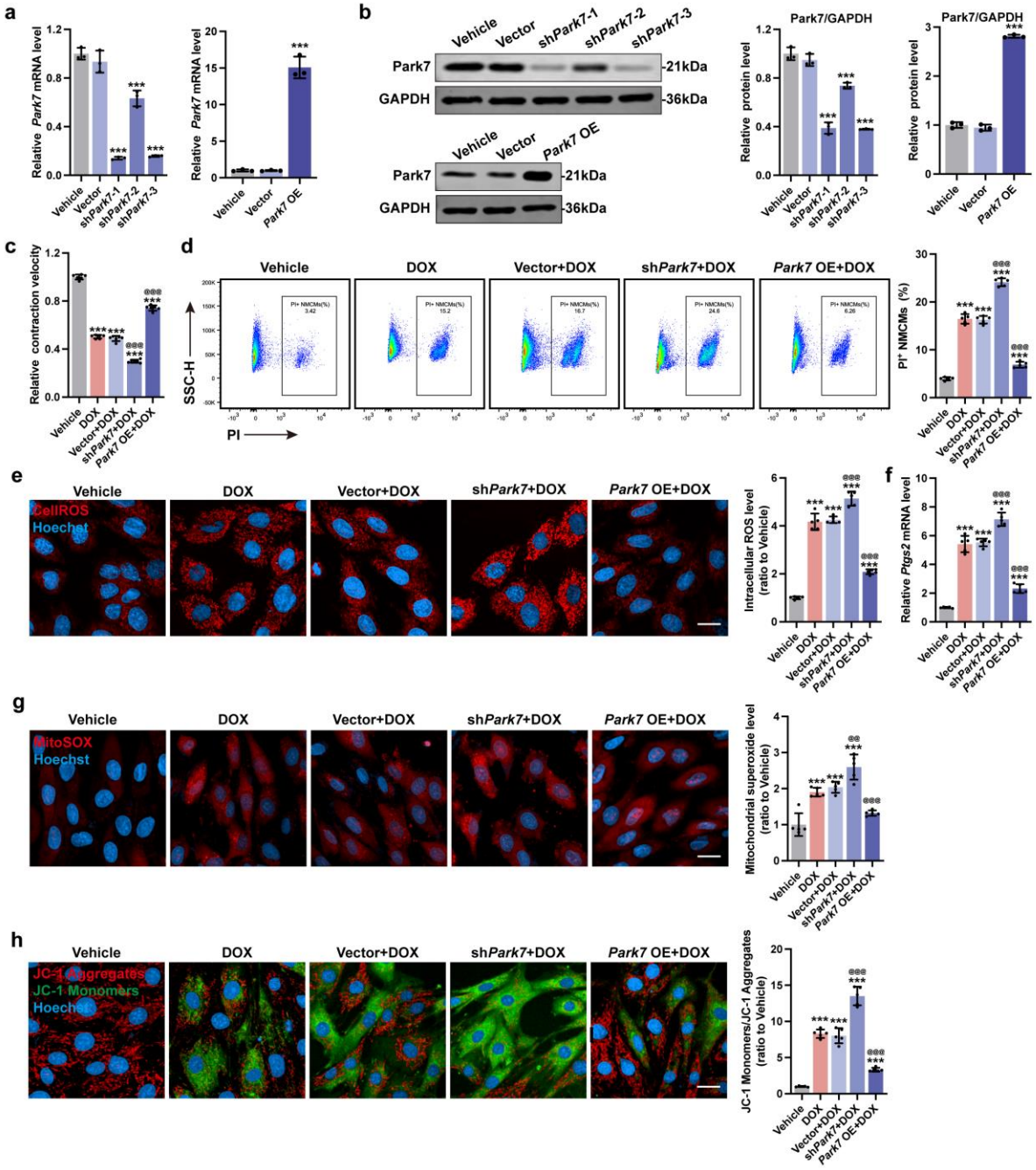

Figure S3 DOX-induced downregulation of Park7 results in loss of iron clearance and promotes mitochondrial iron overload in cardiomyocytes.

a) The infection efficiencies for downregulation or overexpression of *Park7* in NMCMs in mRNA level (n = 5). **b)** The infection efficiencies for downregulation or overexpression of *Park7* in NMCMs in protein level (n = 3). **c)** Contractile velocity of NMCMs extrapolated from live cell imaging (n = 6). **d)** The percentage of PI^+ NMCMs were calculated using flow

cytometry (n = 5). **e)** Representative micrographs and quantification of intracellular ROS (CellROS staining) in NMCMs (scale bars, 20μm; n = 5). **f)** *Ptgs2* mRNA expression level in NMCMs (n = 5). **g)** Representative micrographs and quantification of mitochondrial superoxide level (MitoSOX staining) in NMCMs (scale bars, 20μm; n=5). **h)** Representative micrographs and quantification of mitochondrial membrane potential (JC-1 staining) in NMCMs (scale bars, 20μm; n = 5). The data are expressed as mean ± SD and analyzed using one-way ANOVA followed by Tukey's post hoc test, ***p < 0.001 vs. Vehicle group; @@p < 0.01 and @@@p < 0.001 vs. Vector+DOX group.

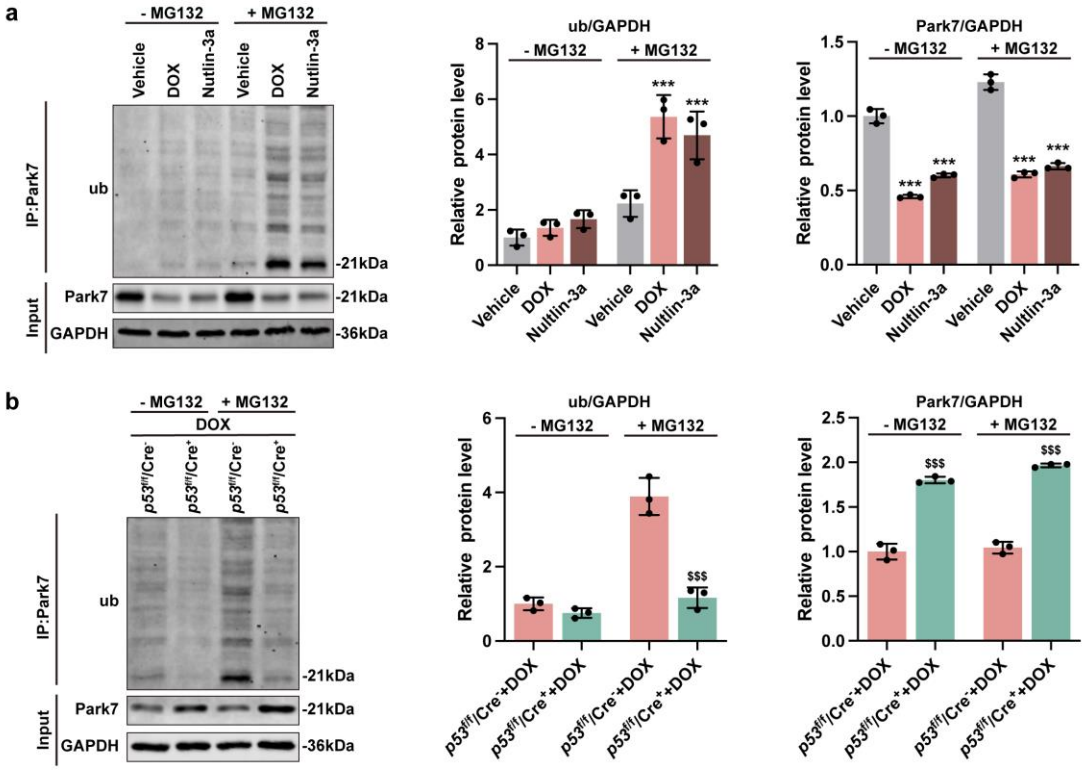

Figure S4 p53 downregulates Park7 protein levels through ubiquitination.

a) MNCMs were treated by DOX or Nutlin-3a with or without MG132 and Park7 was

isolated by IP. Representative immunoblots and quantitative analysis of Park7 ubiquitination were assessed with anti-ub antibody (n = 3). **b)** MNCMs isolated from *p53*$^{f/f}$/Cre^{-} and *p53*$^{f/f}$/Cre^{+} mice were treated by DOX with or without MG132 and Park7 was isolated by IP. Representative immunoblots and quantitative analysis of Park7 ubiquitination were assessed with anti-ub antibody (n = 3). The data are expressed as mean ± SD and analyzed using one-way ANOVA followed by Tukey's post hoc test, ***$p < 0.001$ vs. Vehicle group under the same condition; $$$p < 0.001$ vs. *p53*$^{f/f}$/Cre^{-}+DOX group under the same condition.

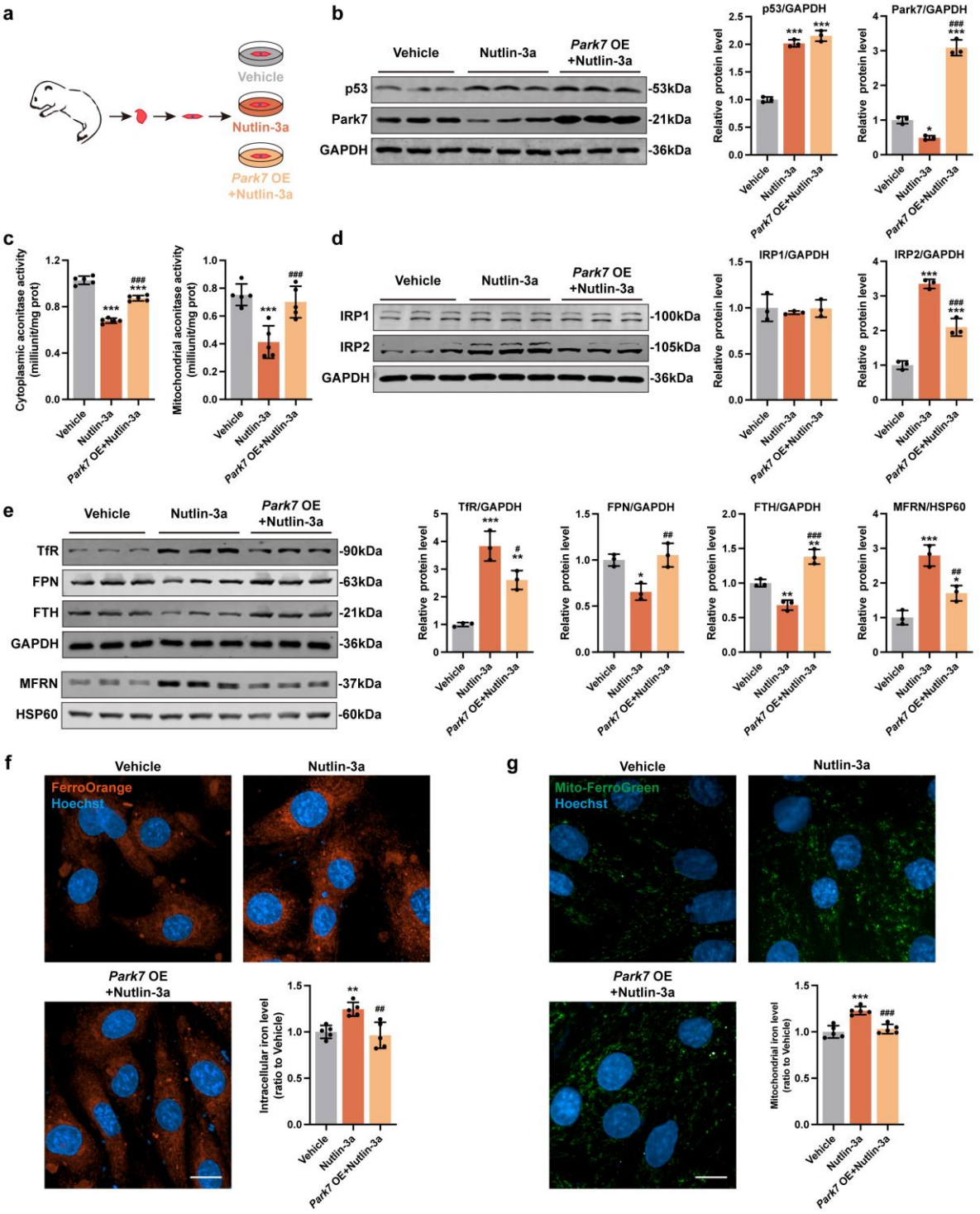

Figure S5 p53/Park7 axis regulates iron homeostasis in healthy cardiomycytes.

a) Experiment design for p53 activation with or without Park7 rescue in healthy NMCMs. **b)** Representative immunoblots and quantitative analysis of Park7 and p53 protein level (n = 3).

c) The cellular aconitase activity and mitochondrial aconitase activity in NMCMs (n = 5). **d)** Representative immunoblots and quantitative analysis of IRP1 and IRP2 protein level in NMCMs (n = 3). **e)** Representative immunoblots and quantitative analysis of iron homeostasis-related proteins in NMCMs (n = 3). **f)** Representative micrographs and quantification of intracellular iron level (FerroOrange staining) in NMCMs (scale bars, 20μm; n = 5). **g)** Representative micrographs and quantification of mitochondrial iron level (Mito-FerroGreen staining) in NMCMs (scale bars, 20μm; n = 5). The data are expressed as mean ± SD and analyzed using one-way ANOVA followed by Tukey's post hoc test, *$p < 0.05$, **$p < 0.01$ and ***$p < 0.001$ vs. Vehicle group; ##$p < 0.01$ and ###$p < 0.001$ vs. Nutlin-3a group.

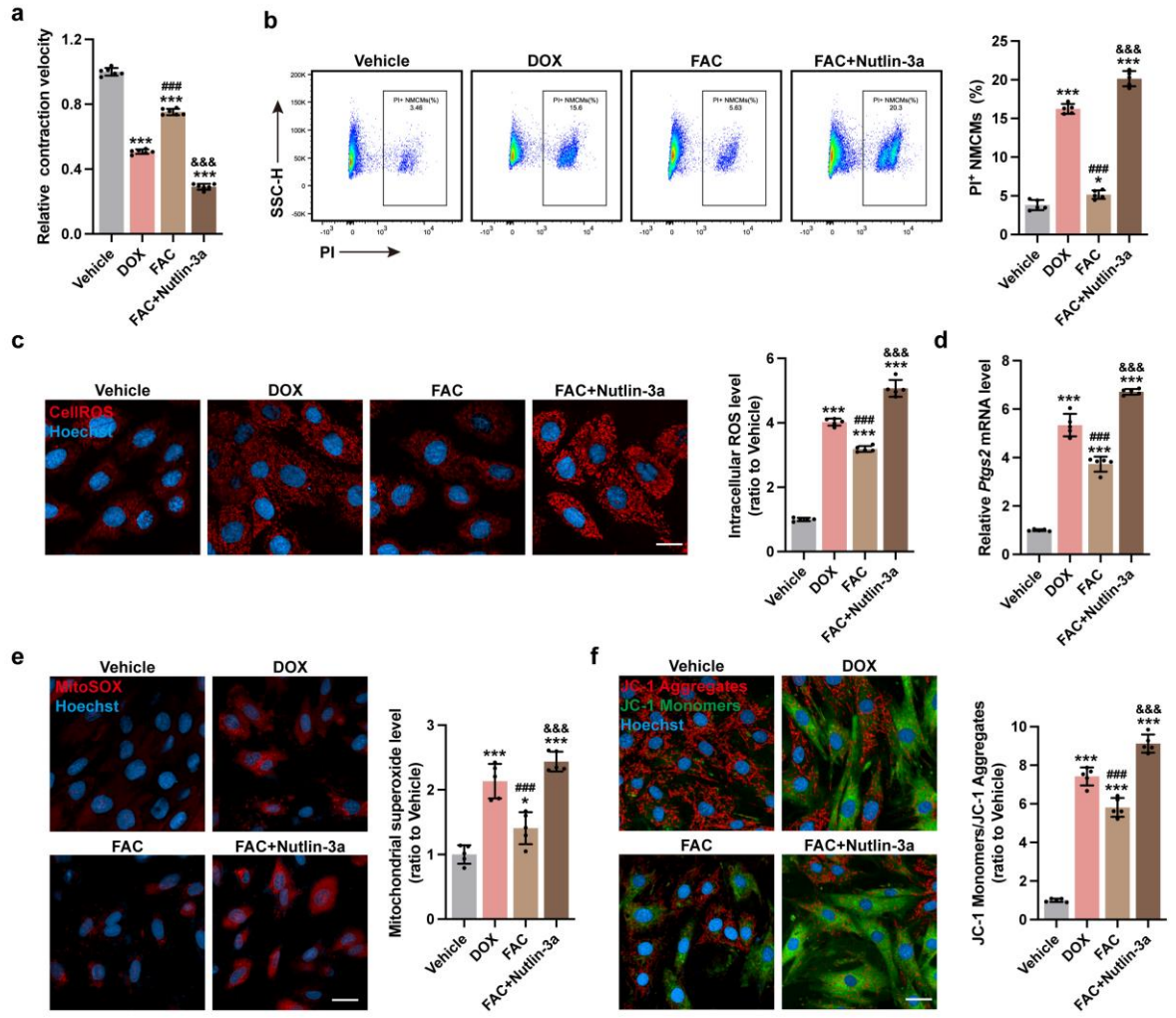

Figure S6 p53 activation recapitulates ferroptosis phenotype in FAC-treated NMCMs.

a) Contractile velocity of NMCMs extrapolated from live cell imaging (n = 6). **b)** The percentage of PI^+ NMCMs were calculated using flow cytometry (n = 5). **c)** Representative micrographs and quantification of intracellular ROS (CellROS staining) in NMCMs (scale bars, 20μm; n = 5). **d)** *Ptgs2* mRNA expression level in NMCMs (n = 5). **e)** Representative micrographs and quantification of mitochondrial superoxide level (MitoSOX staining) in NMCMs (scale bars, 20μm; n = 5). **f)** Representative micrographs and quantification of mitochondrial membrane potential (JC-1 staining) in NMCMs (scale bars, 20μm; n = 5). The

data are expressed as mean ± SD and analyzed using one-way ANOVA followed by Tukey's post hoc test, *p < 0.05 and ***p < 0.001 vs. Vehicle group; ###p < 0.001 vs. DOX group; &&&p < 0.001 vs. FAC group.

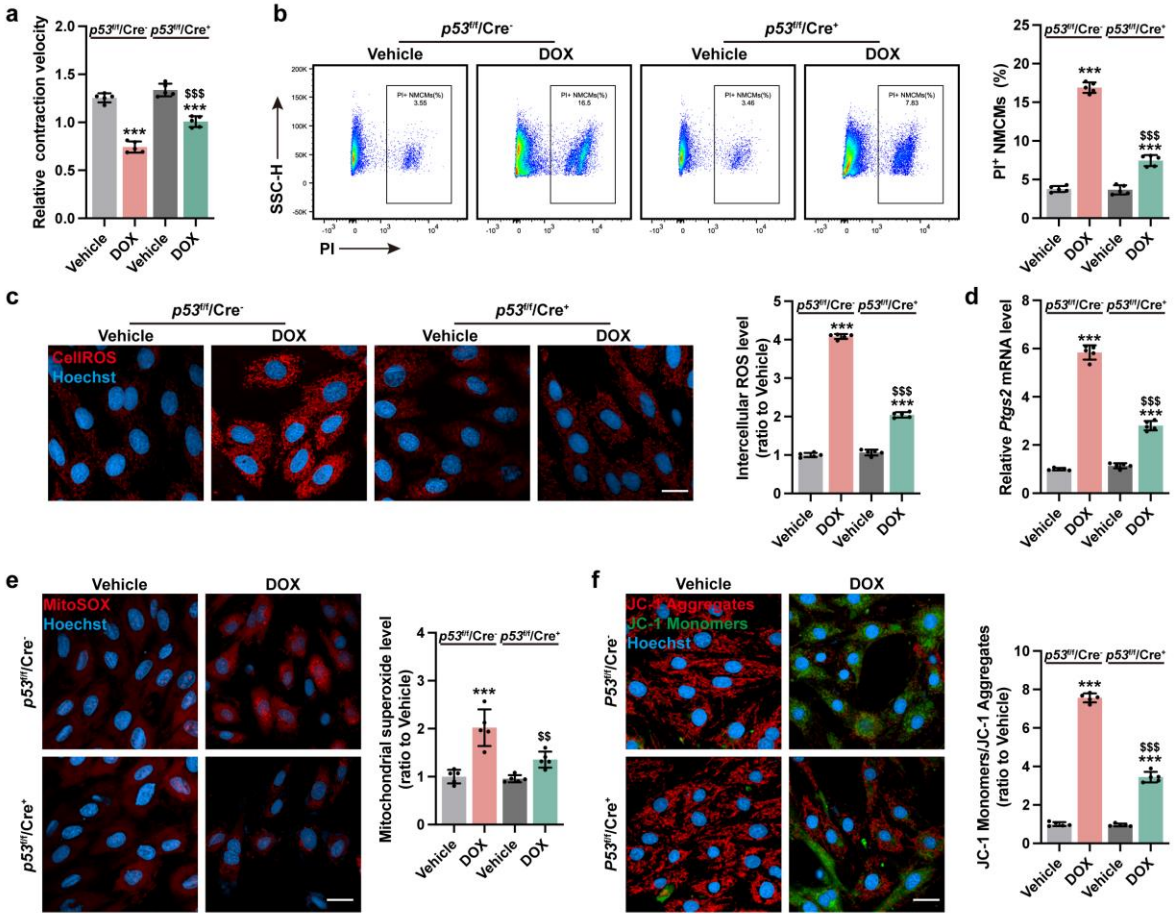

Figure S7 Knockout of *p53* ameliorated DOX-induced iron metabolism dysfunction and ferroptosis in NMCMs.

a) Contractile velocity of NMCMs extrapolated from live cell imaging (n = 6). **b)** The percentage of PI^+ NMCMs were calculated using flow cytometry (n = 5). **c)** Representative micrographs and quantification of intracellular ROS (CellROS staining) in NMCMs (scale bars, 20μm; n = 5). **d)** *Ptgs2* mRNA expression level in NMCMs (n = 5). **e)** Representative

micrographs and quantification of mitochondrial superoxide level (MitoSOX staining) in NMCMs (scale bars, 20μm; n = 5). **f)** Representative micrographs and quantification of mitochondrial membrane potential (JC-1 staining) in NMCMs (scale bars, 20μm; n = 5). The data are expressed as mean ± SD and analyzed using one-way ANOVA followed by Tukey's post hoc test, ***$p < 0.001$ vs. Vehicle group; $$$p < 0.01$ and $$$$p < 0.001$ vs. *p53*$^{f/f}$/Cre^{-}+DOX group.

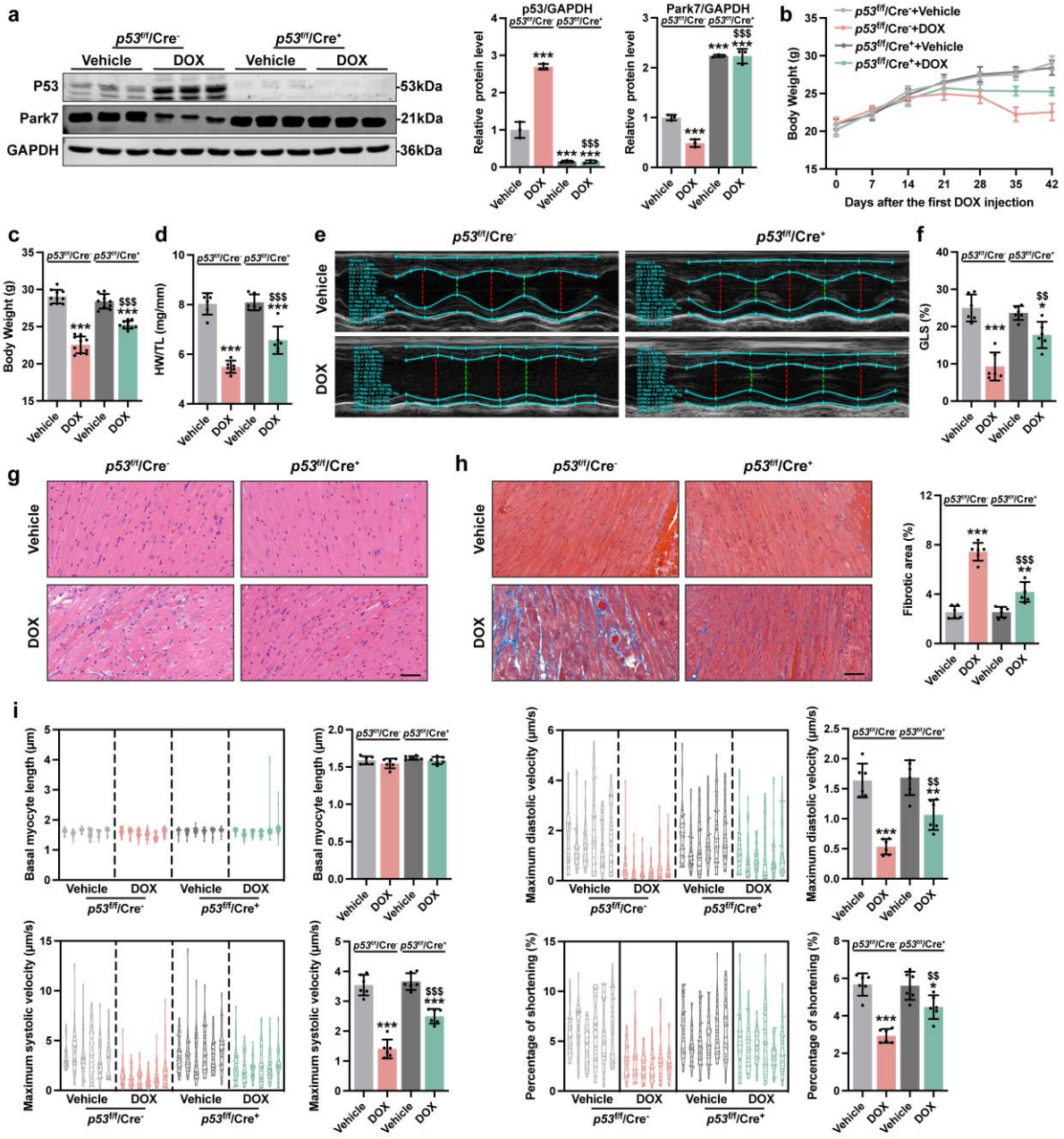

Figure S8 Knockout of *p53* ameliorates DoIC in mice.

a) Representative immunoblots and quantitative analysis of Park7 and p53 protein level in AMCMs (n = 3). **b)** Body weight tracing during DoIC model (n = 10). **c)** Body weight of mice before sacrificed (n = 10). **d)** Ratio of heart weight to tibia length (HW/TL; n = 6). **e)** Representative M-mode images of transthoracic echocardiography**. f)** Quantification of

global longitudinal strain (GLS; n = 6). **g)** Representative micrographs of H&E staining in heart sections (scale bars, 50 μm). **h)** Representative micrographs of Masson's trichrome staining and percentage of fibrotic area in heart sections (scale bars, 50 μm; n = 6). **i)** Calculation of basal myocyte length, maximum systolic velocity, maximum diastolic velocity and percentage of shortening of AMCMs (n = 30 AMCMs per mice, 6mice per group). The data are expressed as mean ± SD and analyzed using one-way ANOVA followed by Tukey's post hoc test, *$p < 0.05$, **$p < 0.01$ and ***$p < 0.001$ vs. Vehicle group; \$\$$p < 0.01$ and \$\$\$$p < 0.001$ vs. $p53^{f/f}$/Cre^{-}+DOX group.

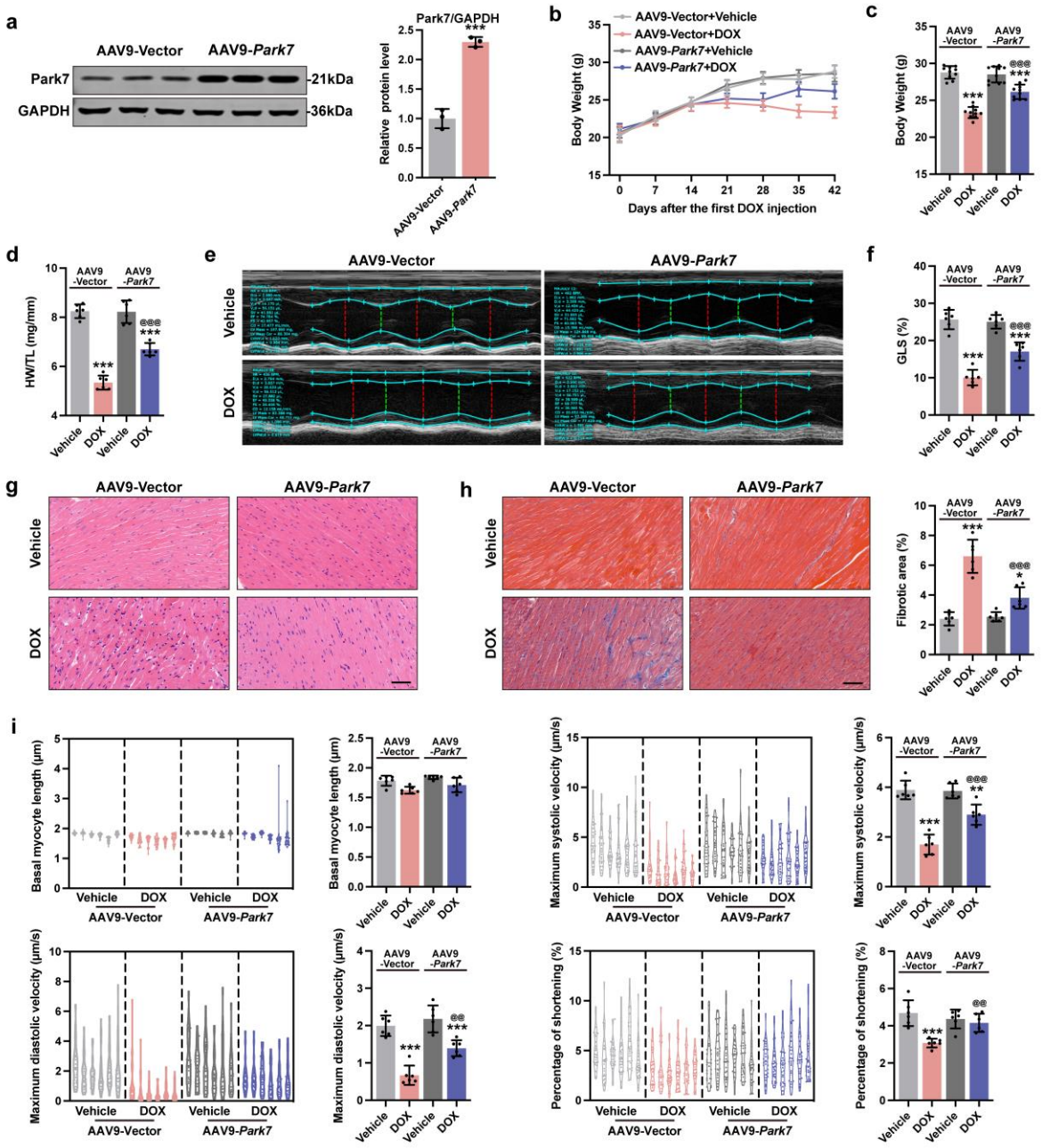

Figure S9 Overexpression of *Park7* ameliorates DoIC in mice.

a) Representative immunoblots and quantitative analysis of Park7 protein level in AMCMs (n = 3). **b)** Body weight tracing during DoIC model (n = 10). **c)** Body weight of mice before sacrificed (n = 10). **d)** Ratio of heart weight to tibia length (HW/TL; n = 6). **e)** Representative M-mode images of transthoracic echocardiography. **f)** Quantification of global longitudinal strain (GLS; n = 6). **g)** Representative micrographs of H&E staining in heart sections (scale

bars, 50 μm). **h)** Representative micrographs of Masson's trichrome staining and percentage of fibrotic area in heart sections (scale bars, 50 μm; n = 6). **i)** Calculation of basal myocyte length, maximum systolic velocity, maximum diastolic velocity and percentage of shortening of AMCMs (n = 30 AMCMs per mice, 6mice per group). The data are expressed as mean ± SD and analyzed using one-way ANOVA followed by Tukey's post hoc test, *$p < 0.05$, **$p < 0.01$ and ***$p < 0.001$ vs. Vehicle group; @@$p < 0.01$ and @@@$p < 0.001$ vs. AAV9-Vector+DOX group.

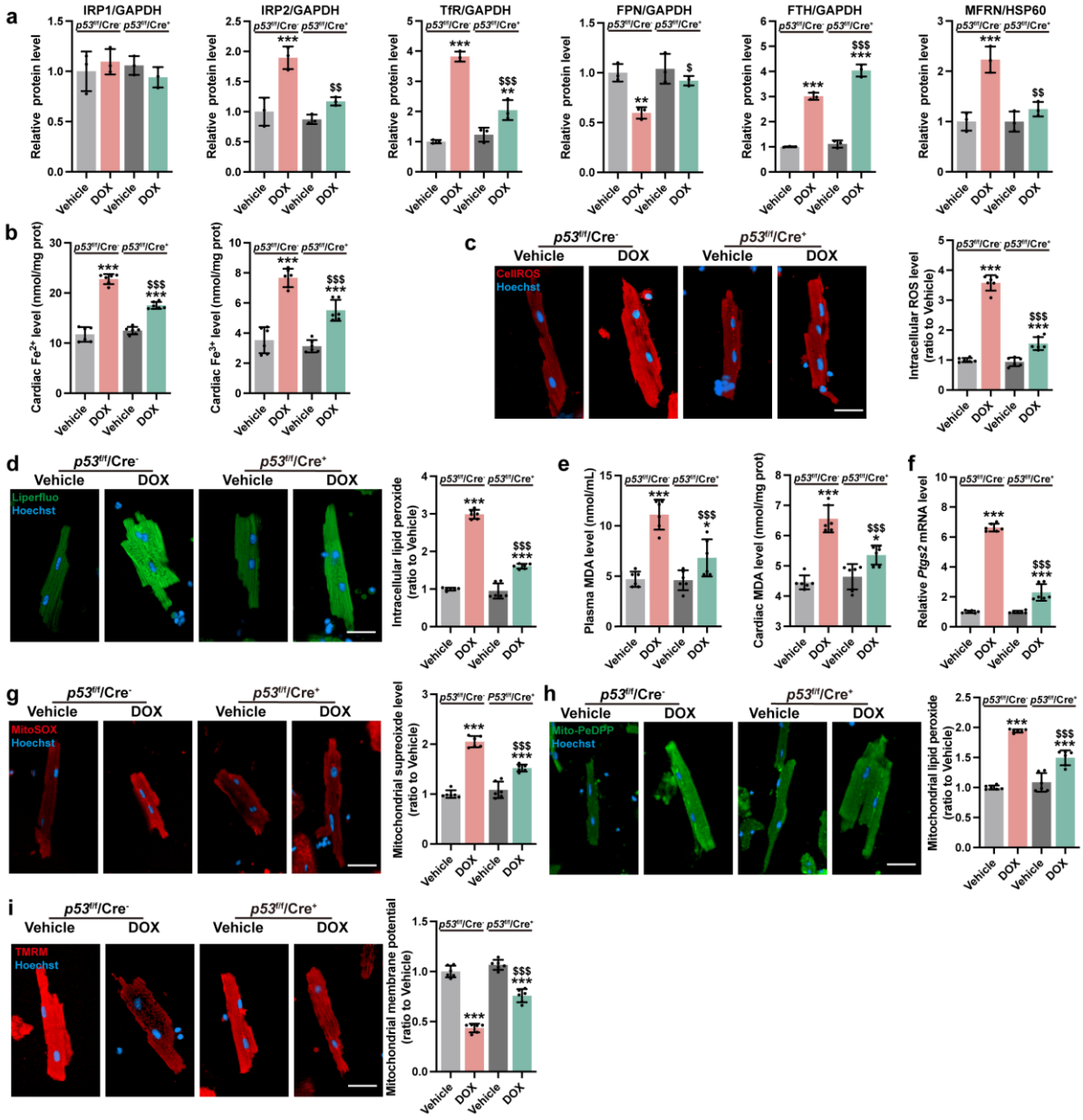

Figure S10 Knockout of *p53* alleviates DOX induced myocardial iron homeostasis dysfunction and ferroptosis in mice.

a) Quantitative analysis of cellular and mitochondrial iron homeostasis-related proteins in AMCMs in Figure 8e (n = 3). **b)** Fe^{2+} and Fe^{3+} levels in heart tissues (n = 6). **c)** Representative micrographs and quantification of intracellular ROS (CellROS staining) in AMCMs (scale bars, 20μm; n = 6). **d)** Representative micrographs and quantification of

intracellular lipid peroxide (Liperfluo staining) in AMCMs (scale bars, 20μm; n = 6). **e)** MDA level in plasma and heart tissues (n = 6). **f)** *Ptgs2* mRNA expression level in AMCMs (n = 6). **g)** Representative micrographs and quantification of mitochondrial superoxide level (MitoSOX staining) in AMCMs (scale bars, 20μm; n = 6). **h)** Representative micrographs and quantification of mitochondrial lipid peroxide (Mito-PeDPP staining) in AMCMs (scale bars, 20μm; n = 6). **i)** Representative micrographs and quantification of mitochondrial membrane potential (TMRM staining) in AMCMs (scale bars, 20μm; n = 6). The data are expressed as mean ± SD and analyzed using one-way ANOVA followed by Tukey's post hoc test, *$p < 0.05$, **$p < 0.01$ and ***$p < 0.001$ vs. Vehicle group; \$$p < 0.05$, \$\$$p < 0.01$ and \$\$\$$p < 0.001$ vs. $p53^{f/f}$/Cre^{-}+DOX group.

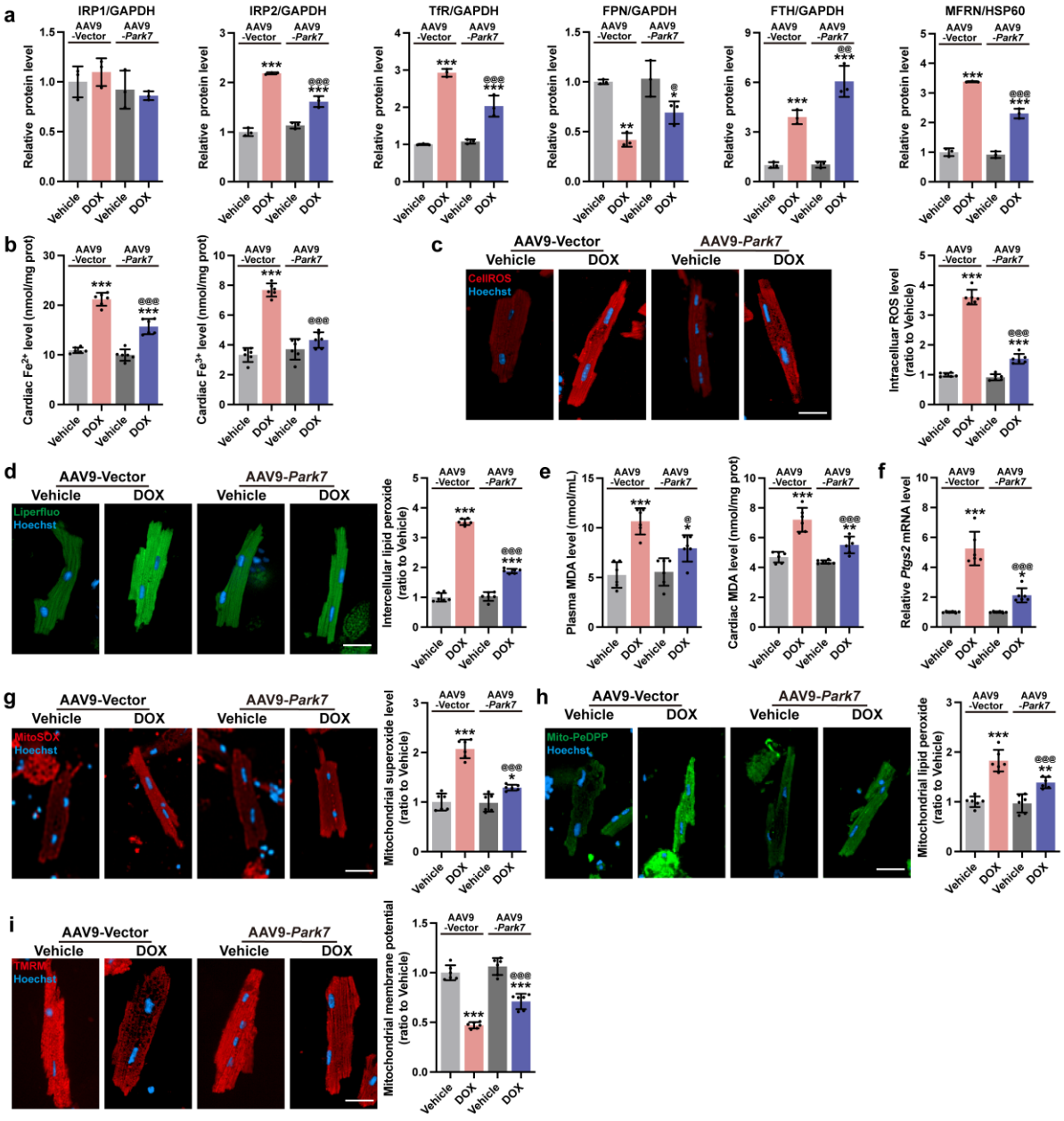

Figure S11 Overexpression of *Park7* alleviates DOX induced myocardial iron homeostasis dysfunction and ferroptosis in mice.

a) Quantitative analysis of cellular and mitochondrial iron homeostasis-related proteins in AMCMs in Figure 8E (n = 3). **b)** Fe^{2+} and Fe^{3+} levels in heart tissues (n = 6). **c)** Representative micrographs and quantification of intracellular ROS (CellROS staining) in AMCMs (scale bars, 20μm; n = 6). **d)** Representative micrographs and quantification of

intracellular lipid peroxide (Liperfluo staining) in AMCMs (scale bars, 20μm; n = 6). **e)** MDA level in plasma and heart tissues (n = 6). **f)** *Ptgs2* mRNA expression level in AMCMs (n = 6). **g)** Representative micrographs and quantification of mitochondrial superoxide level (MitoSOX staining) in AMCMs (scale bars, 20μm; n = 6). **h)** Representative micrographs and quantification of mitochondrial lipid peroxide (Mito-PeDPP staining) in AMCMs (scale bars, 20μm; n = 6). **i)** Representative micrographs and quantification of mitochondrial membrane potential (TMRM staining) in AMCMs (scale bars, 20μm; n = 6). The data are expressed as mean ± SD and analyzed using one-way ANOVA followed by Tukey's post hoc test, *$p < 0.05$, **$p < 0.01$ and ***$p < 0.001$ vs. Vehicle group; @$p < 0.05$, @@$p < 0.01$ and @@@$p < 0.001$ vs. AAV9-Vector+DOX group.